


RESEARCH

Open Access



Structural Behaviour of Polystyrene Foam Lightweight Concrete Beams Strengthened with FRP Laminates

Wael M. Montaser^{1*} , Ibrahim G. Shaaban², Amr H. Zaher³, Sadaqat U. Khan⁴ and Mustafa N. Sayed¹

Abstract

Lightweight concrete (LWC) is one of the most important building materials nowadays. Many research studies were focused on LWC produced using lightweight aggregates. However, limited work was cited for LWC produced using polystyrene beads. In this study, LWC beams strengthened with carbon fibre reinforced polymer (CFRP) and glass fibre reinforced polymer (GFRP) were experimentally tested to investigate the improvement in their flexural and shear behaviours. LWC in this investigation was achieved by partial replacement of normal aggregate by polystyrene beads and resulted in approximately 30% less weight compared to Normal weight concrete. Fourteen Reinforced Concrete (RC) LWC beams of 100 mm by 300 mm cross section having an overall length of 3250 mm were tested under four-point bending. These beams were designed, detailed, and tested to obtain flexural and shear mode of failure. These beams were divided into two groups based on the intended failure mode. In each group, six beams were strengthened using CFRP and GFRP laminates, while the remaining one beam was used as control. The tested parameters were the type of FRP, the width of the laminates used in shear strengthening, and the number of layers used in flexural strengthening. It was found that strengthening of LWC beams using CFRP and GFRP layers resulted in increasing the loading capacity and decreasing deflection as compared to control. The strengthening with CFRP and GFRP is also suitable in reducing the crack width and crack propagation which is more significant in LWC beams. The experimental results were also compared with the expressions in codes for forecasting the strength of LWC beams and it was that these expressions are compatible with the experimental results.

Keywords: lightweight concrete (LWC), polystyrene beads, beam strengthening, advanced composite materials, GFRP, CFRP

1 Introduction

Deterioration of concrete structures and/or changing the function of structures and buildings needs retrofitting and repair of such buildings. Other factors that contribute to the deterioration of civil engineering infrastructure include ageing, poor construction, a lack of maintenance, a change in use, more stringent

design criteria, and natural disasters, such as earthquakes. Strengthening is a promising approach to improve or regain the load-carrying capacity of structures to extend their serviceability (Shaaban & Seoud, 2018). There are many strengthening techniques, such as guniting (Ramesh et al., 2021), jacketing (Maraq et al., 2021), external prestressing (Kim et al., 2021) and fibre reinforced polymer (FRP) (Alhaddad et al., 2021). FRP gained wide acceptance as a promising technique for retrofitting structural members for its high strength to weight ratio, its damping capabilities, its high resistance to corrosion, its fatigue resistance, and the short time scale for repair (Panahi et al., 2021). Glass fibre

Journal information: ISSN 1976-0485 / eISSN 2234-1315

*Correspondence: wmontaser.eng@o6u.edu.eg

¹ Construction and Building Department, Faculty of Engineering, October 6 University, Giza, Egypt

Full list of author information is available at the end of the article



© The Author(s) 2022. **Open Access** This article is licensed under a Creative Commons Attribution 4.0 International License, which permits use, sharing, adaptation, distribution and reproduction in any medium or format, as long as you give appropriate credit to the original author(s) and the source, provide a link to the Creative Commons licence, and indicate if changes were made. The images or other third party material in this article are included in the article's Creative Commons licence, unless indicated otherwise in a credit line to the material. If material is not included in the article's Creative Commons licence and your intended use is not permitted by statutory regulation or exceeds the permitted use, you will need to obtain permission directly from the copyright holder. To view a copy of this licence, visit <http://creativecommons.org/licenses/by/4.0/>.

reinforced polymer (GFRP) and Carbon fibre reinforced polymer (CFRP) are the widely explored types of FRP which have been discussed in the subsequent para.

GFRP inclined strips were used in the shear deficient Normal weight concrete (NWC) beams and they were found effective in arresting the cracks on higher load as compared to control beam (Sundarraja & Rajamohan, 2009). Flexural strengthening of NWC beams using GFRP, CFRP and hybrid FRP sheets was studied (Attari et al., 2012). This research concluded that the use of a two-layer GFRP for strengthening was very efficient as it enhanced the strength capacity by 114%. In another study, NWC beams were strengthened using wrapping of the shear edges of the beams twice at 45° in opposite directions by either CFRP or GFRP and found that the strength increase of the beams strengthened with CFRP was 84% and the displacement reduction was found to be 39.5%. The increase in strength of the beams strengthened with GFRP was 45%, and the deflection reduction was found to be 53.6% (Önal, 2014). Strengthening of NWC beams using FRP was also found to improve the fatigue performance of retrofitted beams by extending the strength and lifetime of the beams (Danraka et al., 2017).

In the last decade, there has been more interest in using lightweight concrete (LWC) in structural members for its reduction of the structural weight while providing suitable thermal insulation (Agrawal et al., 2021). It has many applications including multi-storey buildings, frames, floors, bridges, and prestressed elements of all types. To boost the flexural strength of under-reinforced beams, a series of 40 LWC reinforced beams were strengthened with CFRP. Parameters investigated were reinforcement ratio, CFRP sheet length, CFRP sheet width, beam and half-beam width. The reinforced beams demonstrated a small gain in ultimate load-carrying capacity, as well as a reduction in mid-span deflection. Jacketing was the most successful strengthening strategy in terms of strength augmentation (approximately 41%) when compared to control beam, but it dramatically affected ductility (Shan-nag et al., 2014).

Flexural behavior of concrete strengthened with PU matrix adhesive laminates using small-scale single lap shear specimens, unreinforced flexural specimens, and large-scale RC girders were studied. Experimental results show that although the normal and shear strengths of PU-based adhesives are low, PU-strengthened beams show increased strength and deformability, owing to the load redistribution ability within the bond line (Al-Jelawy & Mackie, 2020).

Bond durability under accelerated environmental conditioning of two FRP systems commonly employed in civil infrastructure strengthening were investigated:

epoxy and polyurethane systems. Five environments were considered under three different conditioning durations (3 months, 6 months, and 1 year).

Results indicate that both epoxy and polyurethane FRP systems do not degrade significantly under environmental exposure. However, flexural tests on the FRP strengthened concrete beams indicate that bond between FRP and concrete shows significant degradation, especially for aqueous exposure (Al-Jelawy, 2013).

Number of different rehabilitation and retrofitting techniques for RC columns reviewed and evaluated. The outcomes can be drawn from the review as follows:

1. Steel jackets provide a passive lateral pressure, similar to the internal transverse reinforcement, which is activated when the column dilates laterally under the effect of axial load.
2. Concrete jackets strengthening technique improves the column axial, shear, flexural strength and stiffness. The bond between the old and new concrete should be enhanced beforehand by roughening the surface of the original member.
3. Ferrocement jacketing technique does not require highly skilled labor. Ferrocement confinement improves ultimate load capacity, resistance to impact, resistance to earthquake, resistance to fire and corrosion, reduces the cost of maintenance.
4. CFRP composite has many advantages compared to other traditional techniques. CFRP sheets have a high strength to weight ratio, very high resistance to corrosion and chemical attacks which makes them, unlike steel plates and concrete jackets, suitable for structures subjected to aggressive environments.
5. GFRPs are great composites for strengthening RC columns. They have shown excellent durability and performance, and they are being widely applied in the construction field because of their light weight and minimal increase in member dimensions (Naji et al., 2021).

Al-Jelawy et al. (Al-Jelawy Haider & Mackie Kevin, 2021) investigated the effect of different environments on the durability and failure modes of two different wet lay-up CFRP systems applied to flexural reinforcement of concrete were investigated: a two-part epoxy and a preimpregnated, water catalyzed polyurethane with aromatic chemistry as a matrix. Durability of concrete, CFRP laminates, and small-scale CFRP-strengthened concrete flexural beams was investigated for each duration (125, 250, and 365 days) and accelerated conditioning environment. Inverse analysis with a numerical model was used to develop conditioned bond-slip models for each composite system. Results and failure modes

of control and conditioned specimens showed that degradation of CFRP-strengthened beams was controlled by the conditioned concrete tensile strength and bond cohesive energy in the epoxy and polyurethane systems, respectively.

Aljaafreh (Aljaafreh, 2016) tested eight LWC beams strengthened using CFRP. It was found that the LWC beams strengthened with the CFRP layer exhibited an appreciable increment in flexural strength compared to the control beam. Similarly, experimental, and analytical results of LWC beams strengthened with GFRP Strips was compared. The results showed that strengthening of Reinforced Concrete (RC) beams by GFRP strips is an effective technique (Kotwal et al., 2017). In 2021, an experimental study was conducted to evaluate the use of FRP-based strengthening procedures to extend the service life of damaged LWC members that had been exposed to intense fires. The heated LWC reinforced beams regained a considerable amount of their load capacity after strengthening and exhibited typical flexural fractures in the bending zone, as well as flexure–shear cracks in the shear span. In addition, it was found that using a single layer and U shaped jacket of FRP sheets at sides and bottom of the beams, was the most effective technique among the others used in their research for regaining their full flexural capacity (Alshannag & Alshenawy, 2021).

LWC and NWC beams were experimentally and numerically tested with U-shaped and closed shape of epoxy-bonded CFRP reinforcement to compare shear-resisting mechanisms between the two beams types. It was found that CFRP can successfully be used in strengthening of LWC beams and the shear strength gained for LWC is less than NWC samples, while modes of failures were almost the same. On the other hand, diagonal shear cracks propagated through the LWC aggregates, while the cracks in NWC were around the aggregates. The numerical results showed that the current design guidelines to estimate the CFRP contribution do not differentiate between concrete types (Al-Allaf et al., 2019).

Partial replacement of normal aggregate by polystyrene beads results in LWC with the benefits of maintaining a reasonable strength, reduced the overall weight of the LWC test beams by approximately 30% compared to their counterparts of NWC beams, low price, and good insulation of polystyrene [Shaaban et al., 2020; Vishakh and Vasudev, 2018]. This is necessary as the use of LWC is increasing day-by-day and the weaker aggregates and interfacial zone of LWC is susceptible for crack propagation and widening (Newman & Owens, 2003). However, we did not cite published work for the LWC beams containing polystyrene beads and strengthened by FRP. Thus,

this study is focusing on the LWC beams containing polystyrene beads and their flexural and shear strengthening using GFRP and CFRP. The parameters of the study are the width of wrapping for shear strengthening and the number of layers for flexure strengthening. The design equations in the codes which were formulated for NWC beams are applied and validated in this investigation for LWC beams containing polystyrene beads and strengthened using FRP laminates.

2 Research Significance

Lightweight concrete is one of the most important building materials that can help to the development of sustainable materials; yet, because of the weaker particles and interfacial zone, crack propagation in LWC beams is relatively faster than in standard concrete beams. As a result, the importance of strengthening LWC beams became apparent. The current study aims to investigate the flexural and shear strengthening using GFRP and CFRP laminates of LWC beams containing polystyrene beads. The existing codes and their design equations for the strengthening of beams using FRP were applied on LWC studied beams containing polystyrene beads. The Comparisons between experimentally obtained loading capacities and those predicted using design codes were carried out.

3 Experimental Program

Total 14 LWC RC beams having dimensions $100 \times 300 \times 3250$ mm were tested under four-point bending. These beams were divided into control, shear and flexure groups, as shown in Table 1. All beams were detailed according to Egyptian Code of Design and Construction of Reinforced Concrete Structures, ECP 203–2018 (ECP, 2018). The dimension, reinforcements and strengthening details of these groups are also mentioned in Table 1. Seven beams (Including one control and Beams in Flexure groups) were detailed in such a manner that intended failure mode was flexure. Beams in Flexure groups were then strengthened for flexure by GFRP and CFRP, as shown in Table 1. On the other hand, the remaining seven beams (Including one control and Beams in shear groups) were detailed in such a manner that the intended failure mode was shear. Fig. 1a, b shows a schematic of reinforcement details of the beams tested for flexure and shear mode of failure, respectively. Two steel types were used, main steel for longitudinal bars of yield tensile strength ($f_y = 360\text{N/mm}^2$) and ultimate tensile strength ($f_{ult} = 520\text{N/mm}^2$) and mild steel for stirrups of yield strength ($f_y = 240\text{N/mm}^2$) and ultimate tensile strength ($f_{ult} = 370\text{N/mm}^2$).

Table 1 Details of beam specimens.

Group	Beam ID	FRP Type	No. of layers at the bottom	FRP Width (mm)	Longitudinal steel		Stirrups		
					Main	Upper	Between loads	Between load & support	
Control	CBS	–	–	–	4Ø18	2Ø12	Ø6@ 140 mm		
	CBF	–	–	–	2Ø10	2Ø10	Ø8@ 200 mm	Ø8@ 100 mm	
Shear group	(1)	GFRP	BGS1	–	30	4Ø18	2Ø12	Ø6@ 140 mm	
			BGS2	–	50				
			BGS3	–	100				
	(2)	CFRP	BCS1	–	30				
			BCS2	–	50				
			BCS3	–	100				
Flexural group	(3)	GFRP	BGF1	1	–	2Ø10	2Ø10	Ø8@ 200 mm	Ø8@ 100 mm
			BGF2	2	–				
			BGF3	3	–				
	(4)	CFRP	BCF1	1	–				
			BCF2	2	–				
			BCF3	3	–				

3.1 LWC Mixes Containing Polystyrene Beads

LWC was obtained by replacing 50% of coarse aggregate with polystyrene beads and adding silica fume to the mix to compensate the weakness of polystyrene (Shaaban et al., 2020). Polystyrene is a petroleum-based plastic made from the styrene monomer and it is known as Styrofoam, which is the trade name of a polystyrene foam product used for housing insulation. Polystyrene is a light-weight material (95% air) and rigid cellular foam. Polystyrene has an excellent resistance to moisture, imperiousness to rot, mildew, and corrosion. In addition, it is a very good electrical insulator, has excellent optical clarity due to the lack of crystallinity, and has good chemical resistance to diluted acids and bases. However, polystyrene brittle and it has poor impact strength due to the stiffness of the polymer backbone. Despite this weakness, styrene polymers are very attractive large-volume commodity plastics. The polystyrene beads are shown in Fig. 2 and their physical properties are reported in Table 2. The mix proportion required by weight for one cubic meter of fresh concrete for the LWC specimens are given in Table 3. Characteristic compressive cube strength, f_{cu} , of the LWC mix was 32 N/mm² is the average strength obtained by testing six cube specimens of 150 × 150 × 150 mm. Six cylindrical Specimens of 150 diameter × 300 mm height, were tested under compression to obtain the stress–strain response. The average cylindrical compressive strength was $f'_c = 27\text{N/mm}^2$. The average density of LWC was 1740 kg/m³.

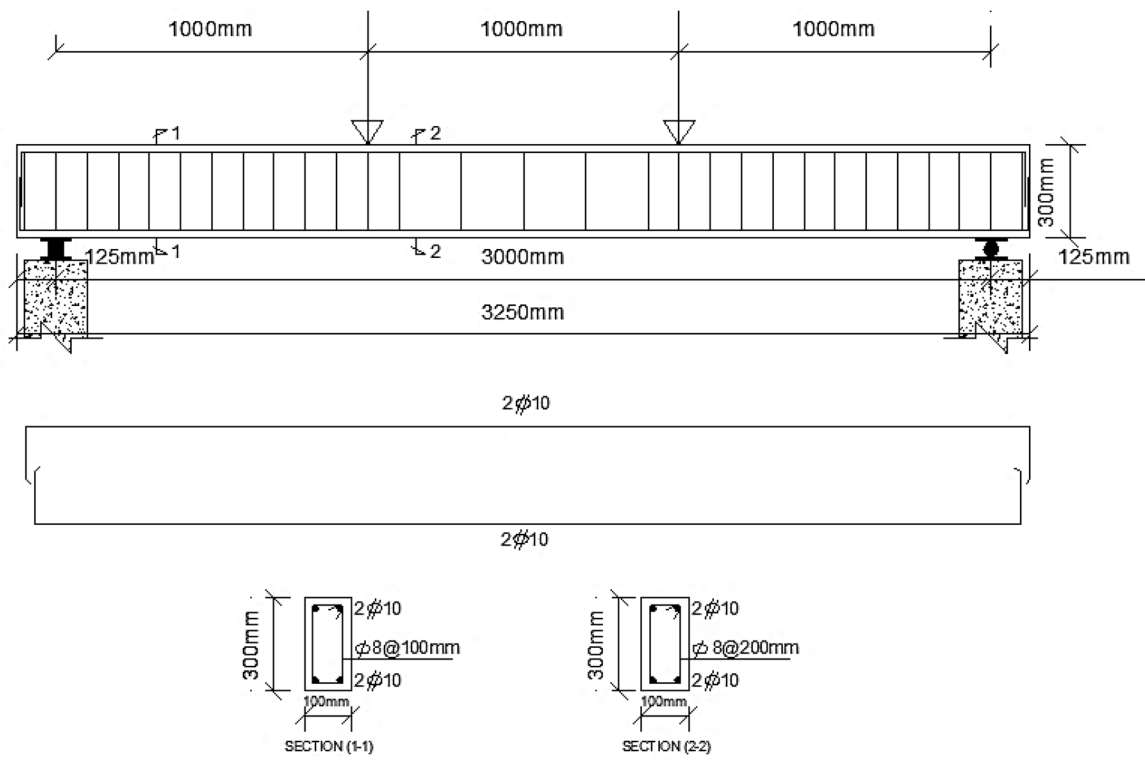
3.2 Beam Fabrication

The formwork made of wood was used for the casting of Beam specimens. The steel reinforcement used in the specimens was prepared and placed in the formwork and the thickness of concrete cover was 2.5 cm (refer to Fig. 3). The beams were cast and compacted for 3 min after casting using an electrical vibrator. The beam surface was levelled to obtain a smooth surface. Samples were cured for 28 days and the curing was carried out by covering the samples with burlap and spraying them with water daily. Strain gauges were embedded in the concrete and mounted on main reinforcement, stirrup reinforcement and longitudinal reinforcement, as shown in Fig. 1a, b.

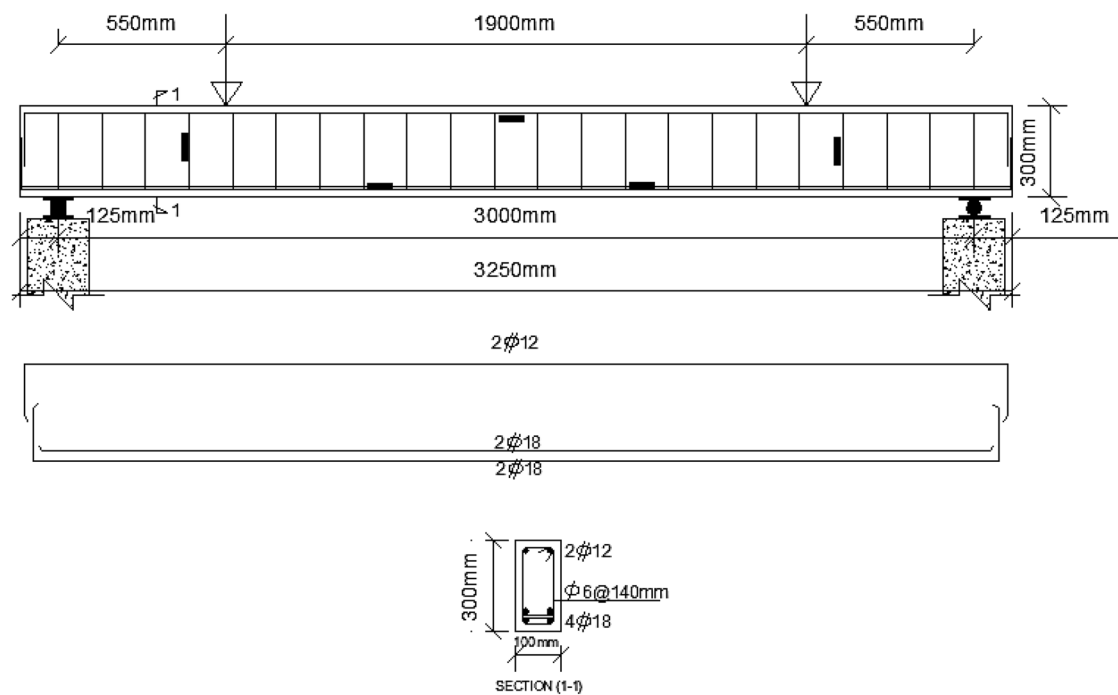
3.3 Steps for Beam Strengthening

GFRP and CFRP layers were attached to the beams after 28 days of casting. The main steps for preparing the surface of beam are as follows:

1. Cleaning the concrete surface using an electrical hand blower to remove the debris on the concrete cover.
2. Application of Epoxy on the concrete surface.
3. Rounding the corners of each beam to a radius of 15 mm.
4. Smoothing the epoxy paste surface.
5. For flexural specimens, attaching the first layer of GFRP or CFRP layers to the bottom surface of the concrete beam with epoxy resin and simultaneously placing subsequent laminates (if appropriate) with



a. Reinforcement details and strain gauges' positions for beams tested in flexure



b. Reinforcement details and strain gauges' positions for beams tested in shear

Fig. 1 Details of beam specimens.



Fig. 2 Polystyrene beads.



Fig. 3 Steel reinforcement of specimens in formwork.

Table 2 Physical properties of polystyrene beads.

Apparent density (kg/m ³)	12.13
Specific density (kg/m ³)	18.5
Compactness (%)	65.57
Porosity (%)	34.43
Thermal conductivity λ (W. m ⁻¹ . K ⁻¹)	0.028
Thermal diffusivity a (mm ² /s)	1.23
Specific heat c (MJ. M ⁻³ . K ⁻¹)	0.022

additional epoxy resin. The fibres orientation of the layer was parallel to the span of the beam (refer to Fig. 4).

6. For shear specimens, wrapping the concrete beam with one layer of U-shaped GFRP or CFRP layers using epoxy resin (refer to Fig. 5).
7. Rolling the FRP layers using a special laminating roller to ensure that the FRP is saturated in epoxy resin and there are no air voids exist between the fibres and concrete surface.

3.4 Testing Setup

Beam Specimens were tested in load control mode using a 1000 kN capacity hydraulic jack with a loading rate of 0.33 kN/s till failure. The load controlled mode was used with slow loading rate as it is suitable for LWC beams as the elastic response is largely



Fig. 4 Attaching the FRP layers on bottom surface of studied beams.

governed in LWC due to its matrix. Above the elastic limit, cracks propagate, which reduces the stiffness of the LWC specimen. This results achieving the peak load and displacement almost at the end of elastic limit with bent-up load–deflection response. The testing setup is shown in Fig. 6. Specimens were instrumented to measure deflection, strain in concrete, strain in transverse reinforcement (stirrups), longitudinal reinforcement strains and crack width synchronised with the applied load. The crack width and deflection were measured using two linear variable displacement transducers (LVDT) 100 mm capacity and 0.001 mm accuracy, as shown in Figs. 7 and 8. The deflections were recorded using three LVDTs which were arranged to measure the deflection distribution. The steel reinforcement strains were measured using five strain gauges.

Table 3 Mix proportion of concrete.

Materi0als	Cement (kg/m ³)	Sand (kg/m ³)	Gravel (kg/m ³)	w/c ratio	Super-plasticize (L/m ³)	Silica fume (kg/m ³)	Polystyrene beads (kg/m ³)
Quantity	450	630	630	0.308	13.5	40	30



Fig. 5 U-shape FRP wrapping.

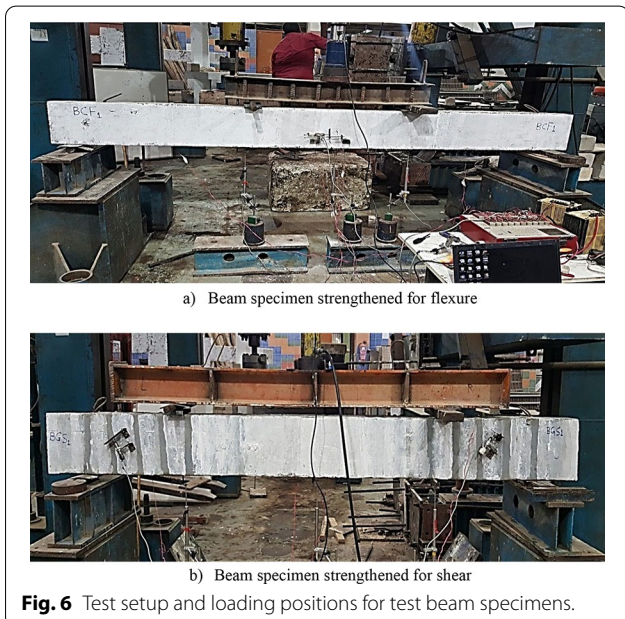


Fig. 6 Test setup and loading positions for test beam specimens.

4 Results and Discussion

4.1 Cracking Loads, Failure Loads, and Crack Pattern

Table 4 presents the failure load and cracking load for shear and flexural cracks. As expected, all the beams detailed as shear deficient were failed in shear before the flexural capacity was reached. While beams in Flexural group were failed in flexure after attaining their capacity. There was no slippage of flexural reinforcement during the testing. As shown in Table 4, the failure load is higher in Shear group and its corresponding control as compared to the failure load in Flexure group and in its control. This is due to the shear span to depth ratio which

is smaller in shear deficient beams. It can also be noticed from Table 4 that strengthening for shear using CFRP resulted in higher loads compared to those of GFRP laminates. In addition, increasing the width of FRP strips for GFRP laminates is more significant than that for CFRP in increasing the failure loads. This is due to the better bonding of GFRP which plays an important role when sufficient width of laminate is provided.

4.1.1 Response of Shear Dominant Specimens

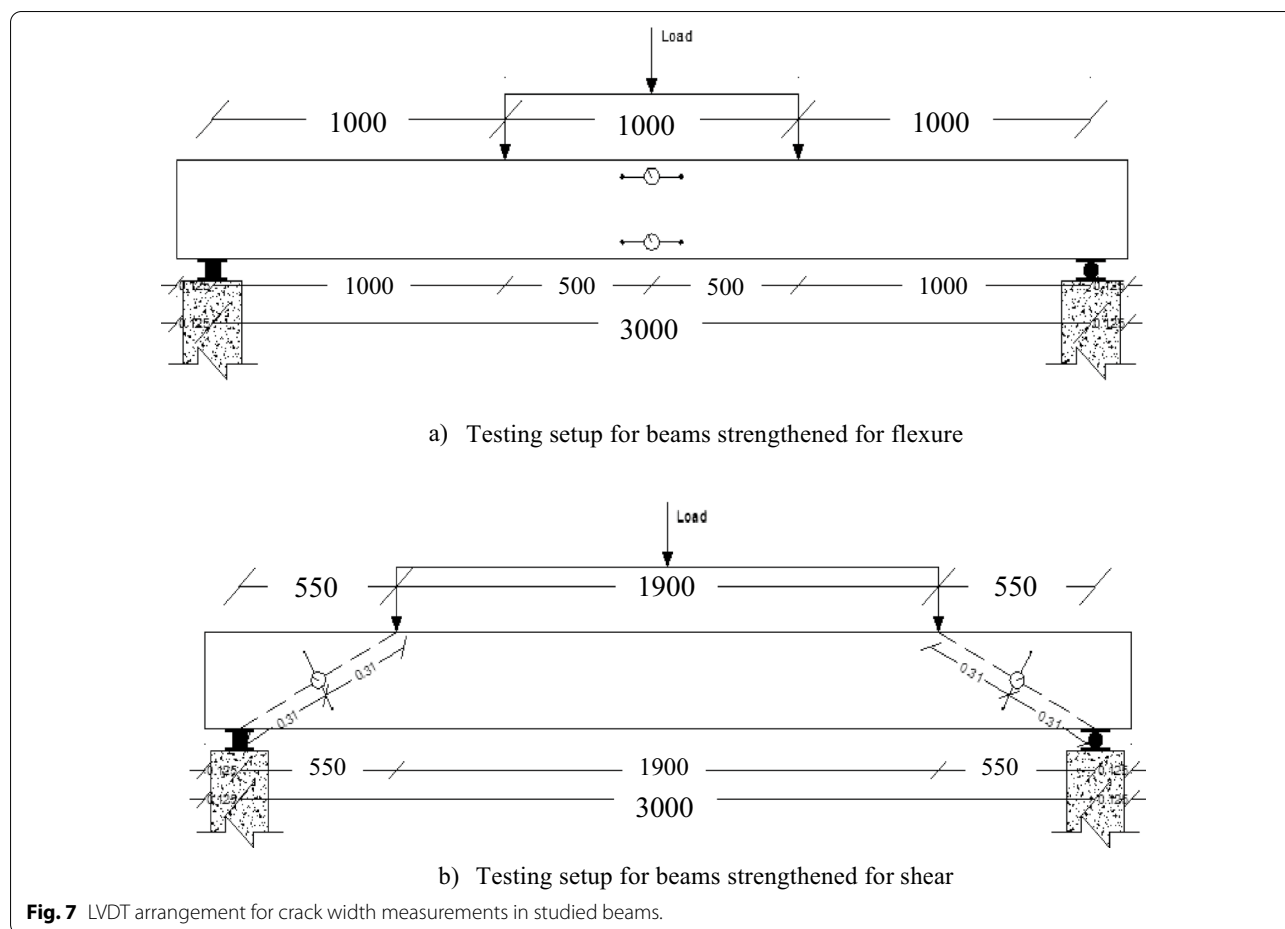
For Group 1, as mentioned in Table 4, the failure load, first shear cracking, and flexural cracking loads for beam BGS1 having 30 mm width of GFRP strip, were higher than those of the control specimen CBS by 13.7%, 57.1%, and 90%, respectively. Increasing the strip width to 50 mm (BGS2), resulted in raising the failure load, first shear cracking, and flexural cracking loads over those of the control specimen CBS by 25.7%, 100%, and 110%, respectively. Similarly, Beam BGS3 having 100 mm width of GFRP strip, increased these loads by 37%, 136%, and 140% as compared to control.

For Group 2, as mentioned in Table 4, the failure load, first shear cracking, and flexural cracking loads for beam BCS1 having 30 mm width of CFRP strip, were higher than those of the control specimen CBS by 20%, 81.4%, and 120%, respectively. Increasing strips' widths to 50 mm (BCS2), resulted in raising the failure load, first shear cracking, and flexural cracking loads over those of the control specimen CBS by 29%, 128.6%, and 150%, respectively. Similarly, Beam BCS3 having 100 mm width of CFRP strip, increased these loads by 50%, 171.4%, and 200%, respectively. The increase in the width of strip of GFRP and CFRP played a dominant role in improving the loading capacity. Shear causes diagonal tension perpendicular to the direction of diagonal crack and increase in the width with fixed length enhanced the tensile capacity of GFRP and CFRP. Therefore, the results are incoherent with the response and propagation of diagonal crack.

4.1.2 Response of Flexural Dominant Specimens

For Group 3, as mentioned in Table 4, the failure load, first shear, and first flexural cracking loads for beam BGF1 having one-layer of GFRP, were higher than those of control specimen CBF by 11.5%, 5.3%, and 0.7%, respectively. Increasing the number of GFRP layers to two (BGF2), resulted in raising the failure load, first shear cracking, and flexural cracking loads over those of the control specimen CBF by 27%, 26.3%, and 19.3%, respectively. Similarly, Beam BGF3 having three layers of GFRP, increased these loads by 50%, 63.2%, and 48%, as compared to control.

For Group 4, as mentioned in Table 4, the failure load, first shear, and first flexural cracking loads for



beam BCF1 having one-layer of CFRP, were higher than those of control specimen CBF by 26.2%, 10.5%, and 6.9%, respectively. Increasing the number of CFRP layers to two (BCF2), resulted in raising the failure load, first shear cracking, and flexural cracking loads over those of the control specimen CBF by 50.5%, 36.8%, and 34.5%, respectively. A further increase of CFRP layers to three (BCF3), increased these loads by 71.5%, 105.3, and 86.2%, as compared to control.

The gain in load carrying capacity after cracking is evident from the above discussion and at the same time there is a deflection-hardening response. Thus, loading capacity along with ductility is enhanced by the strengthening of LWC beam through GFRP and CFRP.

4.1.3 Crack Pattern

The crack pattern was marked to provide the necessary information for defining the failure mechanism of each specimen, as shown in Fig. 9. For beams strengthened for shear, the first diagonal crack suddenly developed at the mid-depth within the shear span. Diagonal cracks were observed parallel to the compression strut, and they

propagated toward the loading region and supports (see Fig. 9). For all flexural specimens, the flexural cracks initiated on the tension side in the mid span of the beam, and the cracks propagated upward with increasing load. All beams strengthened for flexure exhibited flexural failure with peeling out of bottom FRP layers in the specimens BGF1, BGF2, and BCF2, as shown in Fig. 9. This is similar to the study conducted in which peeling out of layers of CFRP in some of their NWC concrete specimens strengthened with CFRP laminates for flexure was observed (Valivonis & Skuturna, 2007). However, the loading capacity and deflection-hardening response was observed in all beams strengthened for flexural failure. This infers that the peeling out of FRP layers do not hinder in attaining the ductile response of LWC beam strengthened through FRP.

4.2 Load–Deflection Response

The load–deflection curves for all the beams are shown in Fig. 10. The load–deflection was approximately linear from zero-load to crack initiation in all the beams. The

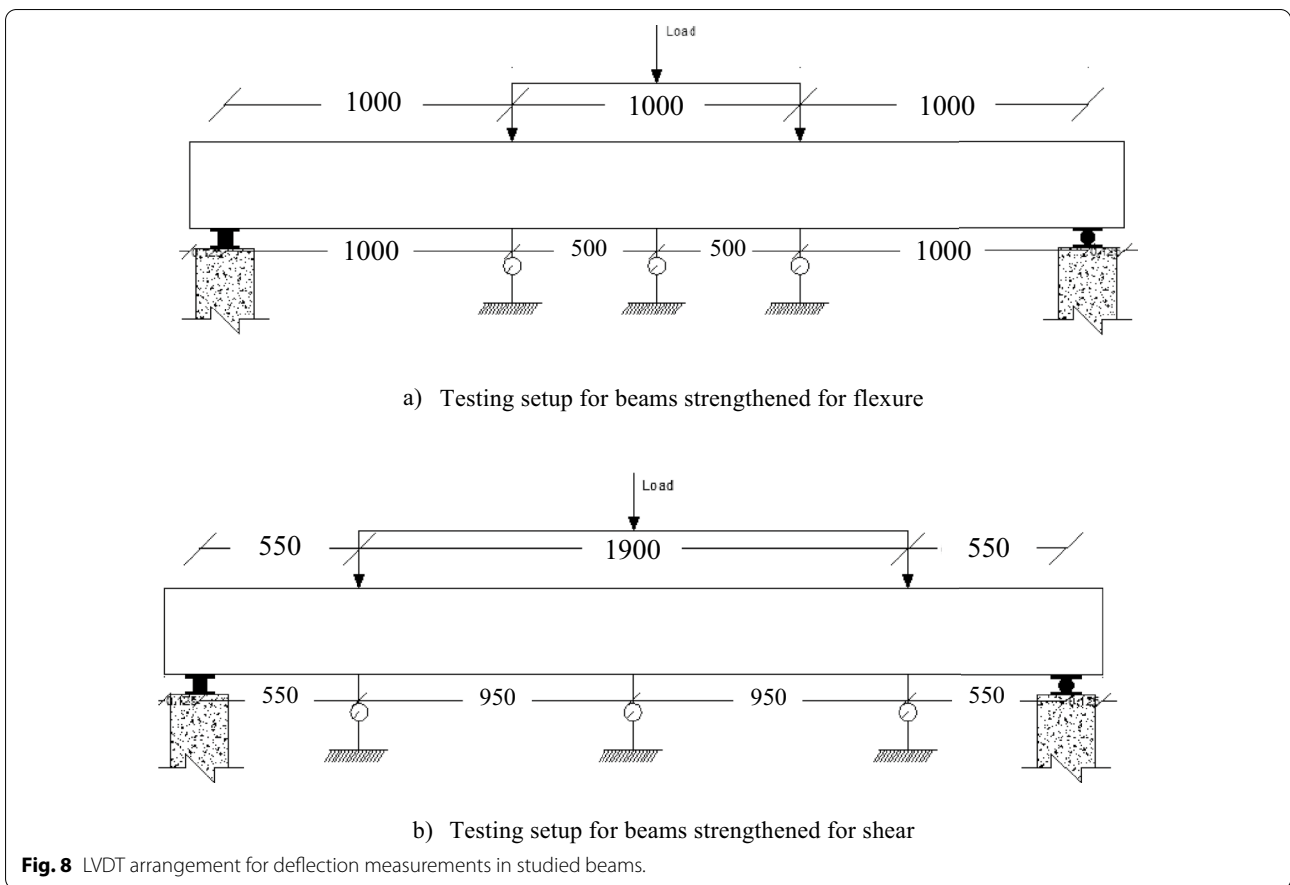


Table 4 Load at first shear crack, first flexural crack and at failure.

Group	Specimen	Failure load (kN)	First shear cracking load (kN)	First flexural cracking load (kN)	Percentage Load carried from first crack to failure (%)	
Control	CBS	173	70	50	71	
	CBF	44.2	19	14.5	67.2	
Shear groups	Group 1	BGS1	196.7	110	95	51.7
		BGS2	217.4	140	105	51.7
		BGS3	237.3	165	120	49.4
	Group 2	BCS1	207	127	110	46.9
		BCS2	223.2	160	125	44
		BCS3	259.6	190	150	42.2
Flexural groups	Group 3	BGF1	49.3	20	14.6	70.4
		BGF2	56.1	24	17.3	69.1
		BGF3	66.1	31	21.5	67.5
	Group 4	BCF1	55.8	21	15.5	72.2
		BCF2	66.5	26	19.5	70.7
		BCF3	75.8	39	27	64.4

large reduction in stiffness caused by excessive cracking resulted in a relatively large increase in the deflection values. Closing to the failure load, the deflection continued to increase, even when the applied load was constant.

Fig. 10 shows that the stiffness and load carrying capacity was increased by increasing the width of FRP strips for shear strengthening or increasing the number of FRP layers for flexural strengthening. Beam specimens BGS1, BGS2 and BGS3 were strengthened via surface attachment of U-shaped GFRP laminates with widths of 30, 50, and 100 mm, respectively. Fig. 10a shows that the load carrying capacity of specimens BGS1, BGS2 and BGS3 were higher than that of CBS control specimen;

however, the deflection was lesser at the same load level for beams BGS1, BGS2 and BGS3 by approximately 11%, 18% and 28%, respectively. Beam specimens BCS1, BCS2 and BCS3 were strengthened via surface attachment of U-shaped CFRP laminates with widths of 30, 50, and 100 mm, respectively. Fig. 10a shows that the load carrying capacity of specimens BGS1, BGS2 and BGS3 were higher than that of CBS control specimen; however, the deflection was lesser at the same load level for beams BCS1, BCS2 and BCS3 by approximately 18%, 35% and 40%, respectively. It can be observed that there is an improvement in stiffness as a result of increasing the FRP strip width from 30 to 100 mm regardless the type of

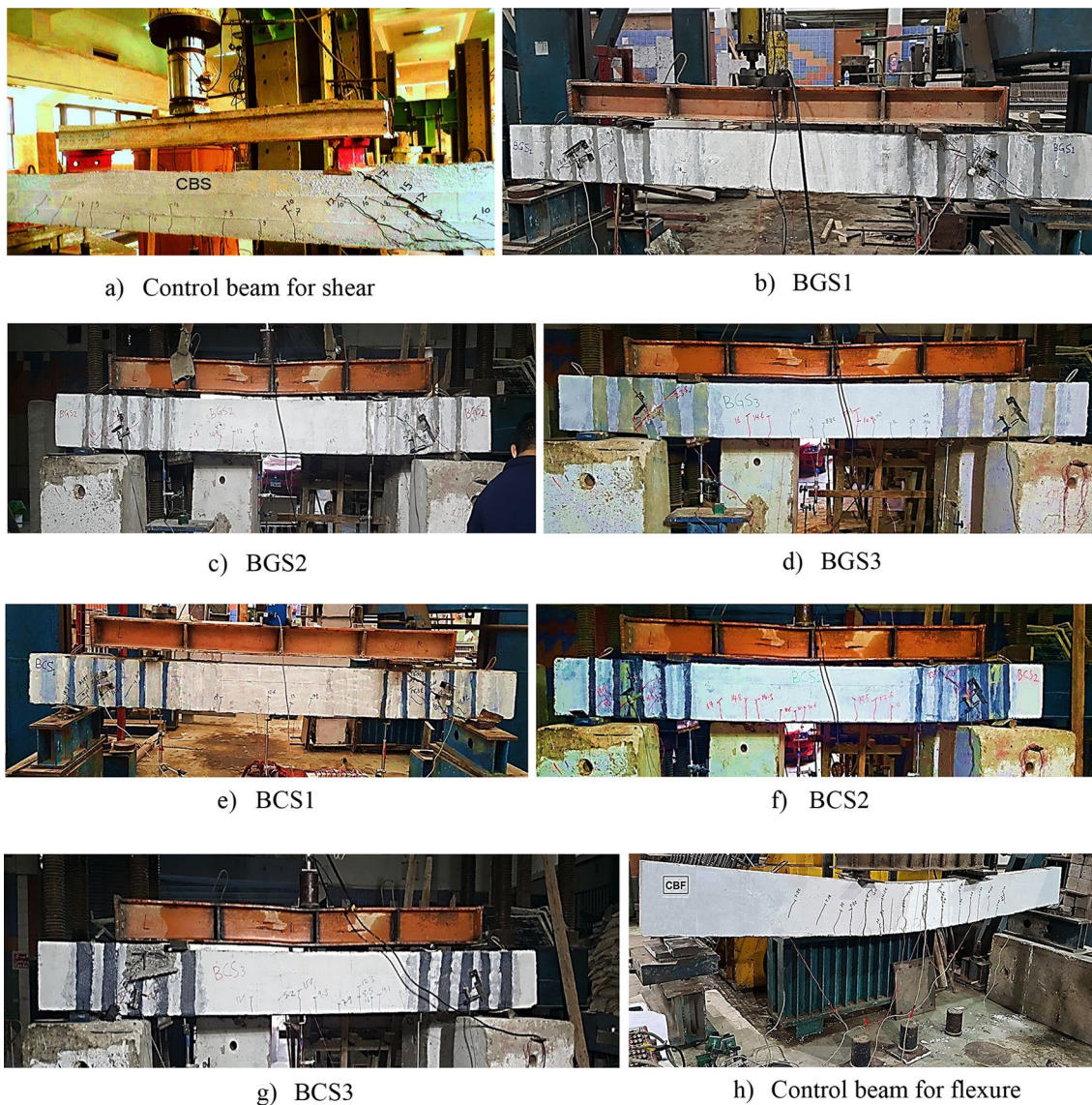


Fig. 9 Crack patterns of all beam specimens.



Fig. 9 continued

FRP. However, the effect of increasing the width of CFRP strengthening strips on the stiffness of the studied beams is slightly higher than that for GFRP strips. To take maximum advantage of FRP strengthening, it is recommended to employ the maximum width of FRP for strengthening LWC beams for shear.

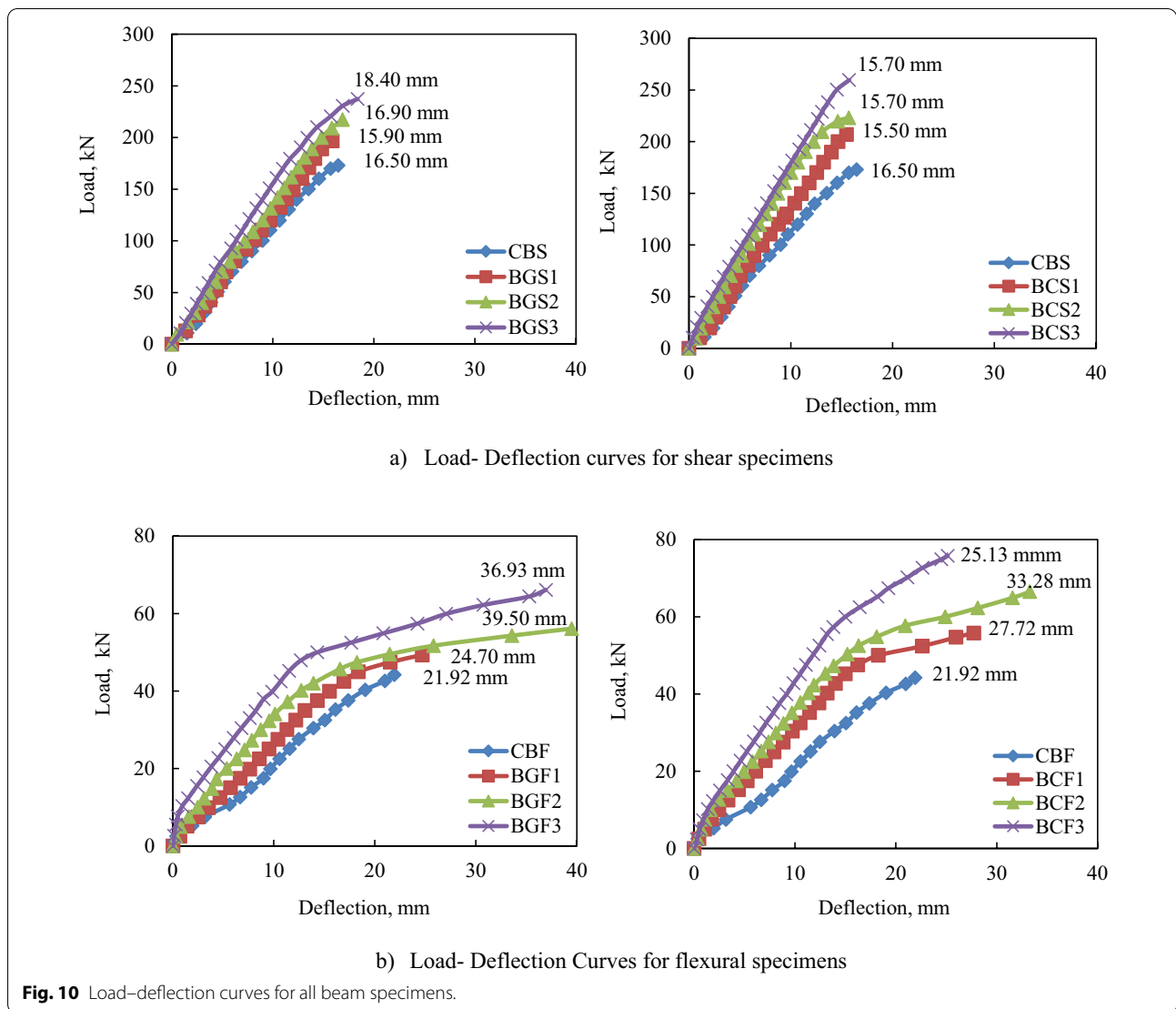
Fig. 10b shows that beam specimens BGF1, BGF2, and BGF3 were strengthened by attaching one, two and three layers of GFRP laminates to the bottom surface of each specimen. The load carrying capacity of specimens of BGF1, BGF2 and BGF3 specimens were higher than that of CBF control specimen; however, the deflection was lesser at the same load level for beams BGF1, BGF2 and BGF3 by approximately 18%, 33% and 48%, respectively. Beam specimens BCF1, BCF2 and BCF3 were strengthened by attaching one, two and three layers of CFRP laminates to the bottom surface of each specimen. The load carrying capacity of specimens of BCF1, BCF2 and BCF3 specimens were higher than that of CBF control specimen; however, the deflection was lesser at the same load level for beams BCF1, BCF2 and BCF3 by approximately 30%, 40% and 52%, respectively. Based on these results, it is inferred that there is an improvement in stiffness as a result of increasing the FRP strengthening layers. However, the effect of increasing the number of CFRP layers on the stiffness is more significant than that for GFRP layers. As a result, this strengthening technique reduces

or eliminates the rate of crack formation, delays initial cracking, reduces stiffness degradation with residual deflection, and extends the fatigue life of LWC beams. CFRP is the greatest alternative for strengthening LWC beams.

4.3 Crack Width

The crack width was measured using LVDTs, as shown in Fig. 11. By comparing the crack widths of the tested beams at the same load level, it was observed that the crack width was decreased with increasing the width of strips or the number of strengthening layers.

For Shear strengthened beams, the crack widths of beam specimens BGS1, BGS2 and BGS3 were less than that of CBS control specimen at the same load by approximately 26%, 38% and 45%, respectively. Similarly, the crack widths of BCS1, BCS2 and BCS3 specimens were less than that of CBS control specimen at the same load level by approximately 32%, 51% and 58%, respectively. For Flexural strengthened beams, the crack widths of BGF1, BGF2 and BGF3 specimens were less than that of CBF control specimen at the same load level by approximately 9%, 18% and 37%, respectively. Similarly, the crack widths of BCF1, BCF2 and BCF3 specimens were less than that of CBF control specimen at the same load level by approximately 24%, 35% and 48%, respectively.



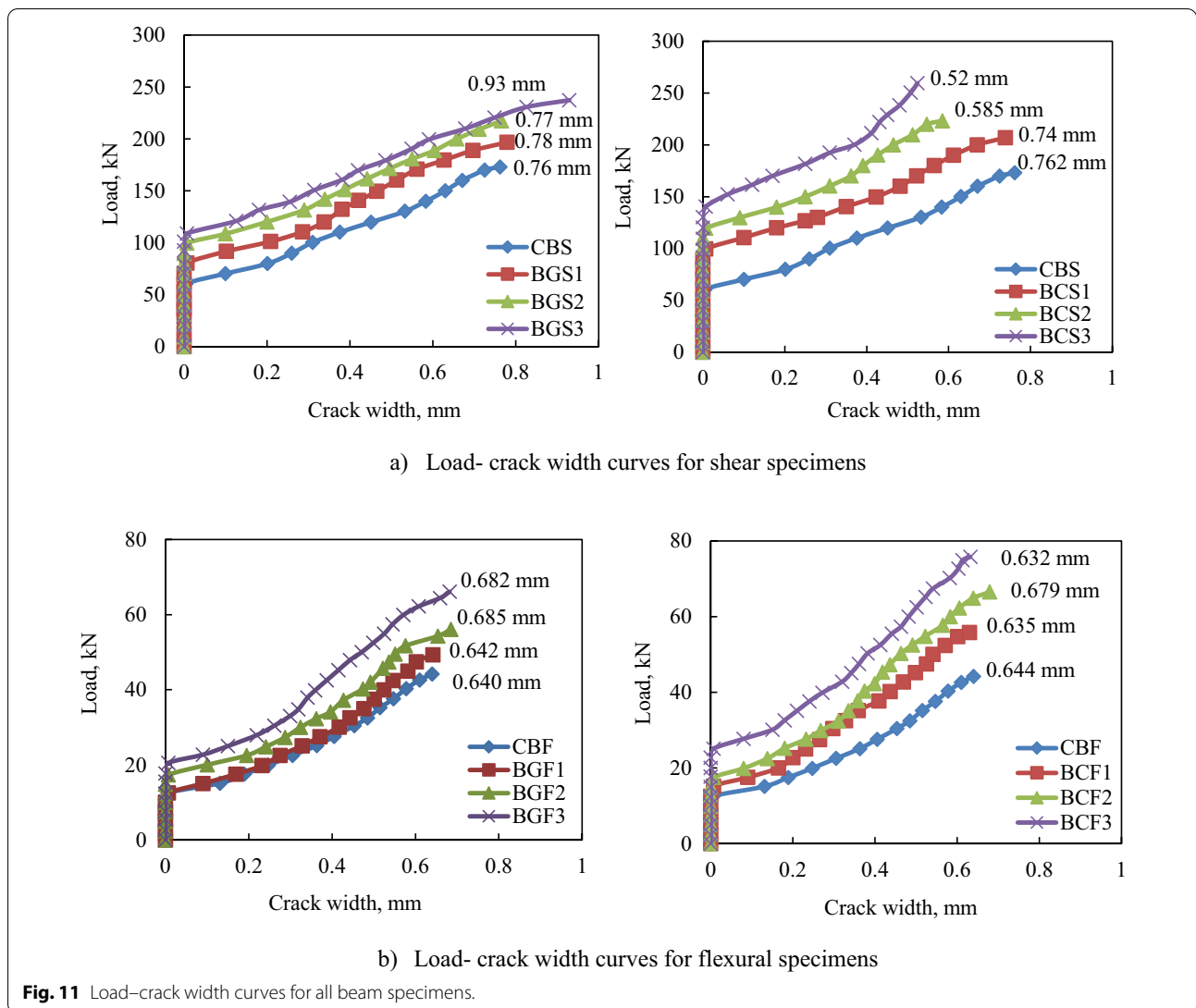
These results also show that the crack width was decreased due to the increase in the overall beam stiffness as a result of increasing the width of FRP strips or increasing the number of FRP strengthening layers. It can also be observed that Shear strengthened beams with CFRP laminates generally had less crack width as compared to the beams strengthened using GFRP laminates. The crack width was almost zero in the elastic range of LWC beams strengthened through FRP, as shown in Fig. 11, this is important as reducing the crack width also limit the exposure of reinforcement to the deleterious substances, such as chloride and sulphates. The reduction in crack width is also depending on the steel strain which is directly proportional with the crack width. The effect on the steel strain through FRP a is discussed as under:

4.4 Steel Strain

Fig. 12 shows the strain at steel level measured through electrical strain gauges mounted on the beam longitudinal reinforcement and stirrups.

4.4.1 Strain at Longitudinal Reinforcement Level

Fig. 12a shows the load vs strain at longitudinal steel level for shear strengthened beams. It is evident that the strain was increased after strengthening and it depends upon the widths of strengthening strips. The strains at failure were below the strain at yielding point of steel. This shows that the shear strengthened beams were failed on the higher load, but the mode of failure was compression rather than yielding. Strengthening with CFRP has a higher effect on the steel strains compared



with strengthening with GFRP. In addition, the effect of increasing the widths of CFRP strengthening strips on the longitudinal steel strains was more significant than for GFRP strips. Fig. 12b shows the load vs strain at longitudinal steel level for flexural strengthened beams. It is evident that the strain was increased after strengthening and it depends upon the number of layers of laminates. The strains at failure were higher than the strain at yielding point of steel. This shows that the flexural strengthened beams were failed on the higher load with the mode of failure was tension. Strengthening with CFRP has a higher effect on the steel strains compared with strengthening with GFRP. In addition, the effect of increasing the number of CFRP layers on the longitudinal steel strains was more significant than for GFRP layers.

Based on the preceding discussion, it is clear that FRP strengthening does not change the mode of failure; rather, the increased strain, number of fractures, and loading capacity indicate that LWC beams are exhibiting symptoms prior to failure. This is especially crucial for shear deficient LWC beams to show signs of failure before approaching the brittle failure phase.

4.4.2 Strain at Stirrups Level

Fig. 13 shows the steel strains in the stirrups of the tested beams at the same load level. The steel strains in the stirrups dropped when the widths of strengthening FRP strips or the number of strengthening FRP layers increased, as shown in the figure.

Fig. 13a demonstrates that the stirrup steel strains of BGS1, BGS2, and BGS3 specimens were smaller than

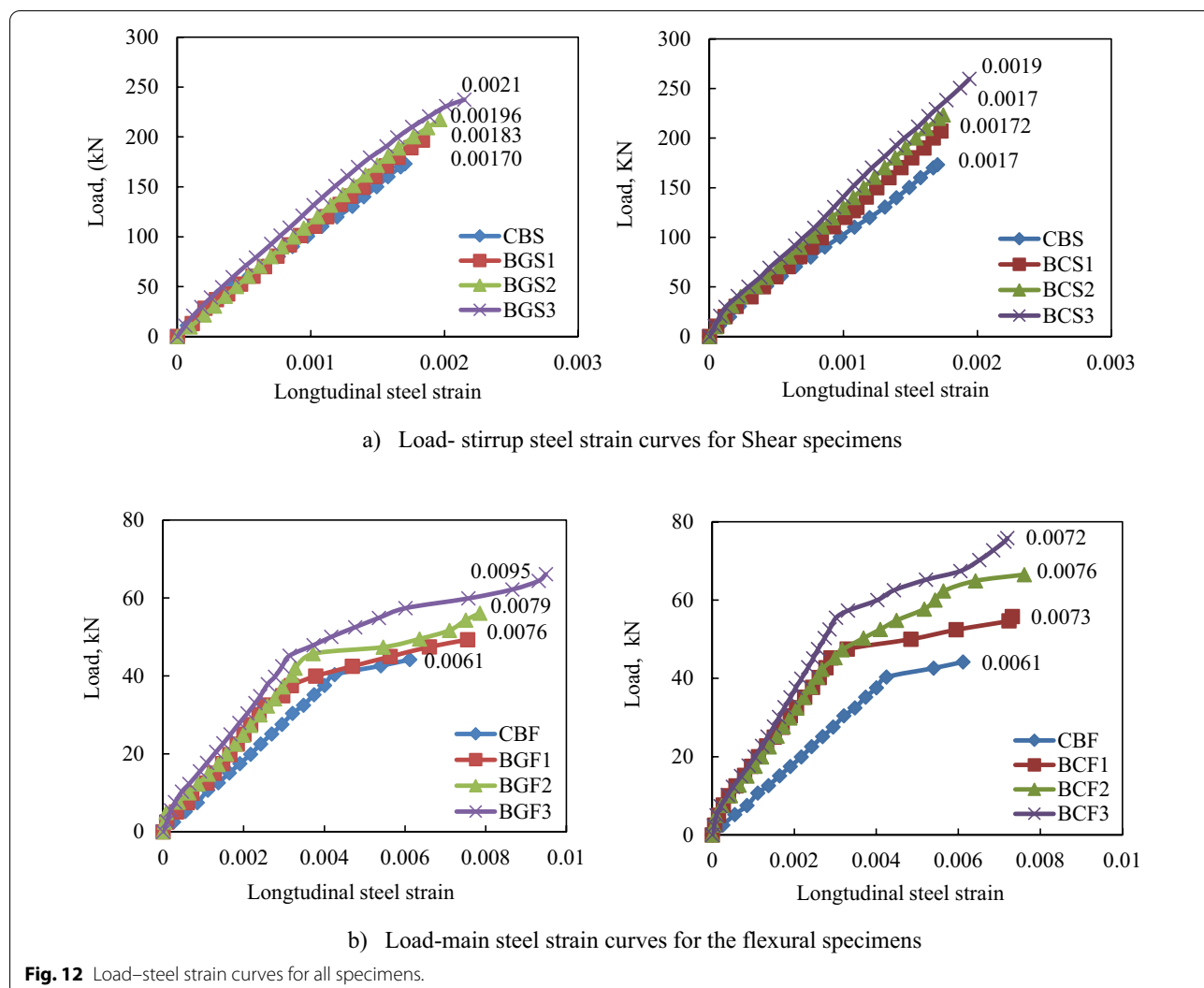


Fig. 12 Load–steel strain curves for all specimens.

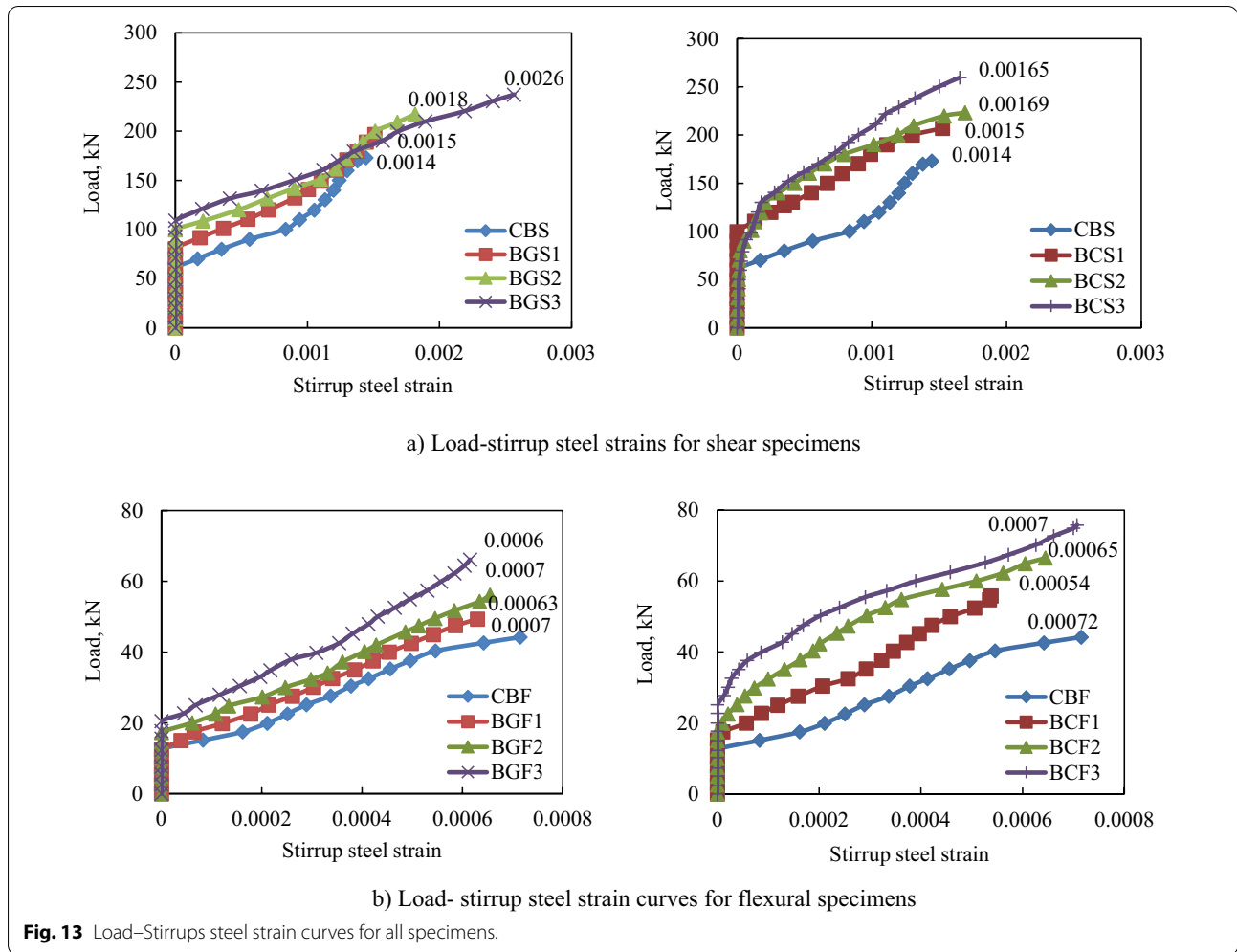
that of CBS control specimens at the same load level by approximately 7%, 11%, and 18%, respectively, for beams strengthened for shear. Furthermore, at the same load level, the steel strains of BCS1, BCS2, and BCS3 specimens were roughly 46%, 65%, and 71% lower than the CBS control specimen. It's worth noting that the reduction in stirrup strain caused by CFRP strip stiffening is nearly 7 times more than that caused by GFRP strip stiffening. For GFRP laminates; however, increasing the strip width from 30 to 100 mm had a greater impact.

Fig. 13b shows that the steel strains of the stirrups of BGF1, BGF2, and BGF3 specimens were lower than those of the CBF control specimen at the same load level by about 16%, 25%, and 43%, respectively, for beams strengthened for flexure. The steel strains of the BCF1, BCF2, and BCF3 stirrups, on the other hand, were roughly 36%, 65%, and 84% lower than the CBF control specimen at the same load level. The difference between

the two FRP types on the stirrup's strains is less than the difference between the other examined parameters in the preceding sections, as can be seen from the above values. It may conclude that the number of layers is more effective for GFRP laminates as compared to CFRP. However, all beams strengthened through GFRP and CFRP demonstrate deflection-hardening, reduction in crack width, and longitudinal steel strains.

5 Comparison of Experimental and Analytical Results

In the following sections, the predictive equations specified in design codes were used and compared with the ultimate load capacity of beams strengthened with FRP laminates. These equations are primarily developed for normal weight concrete and comparison of the predictive loads with the lightweight concrete beams was performed in this study. The idea is to highlights the shortcomings in



the existing equations and check whether these can serve for designing LWC beams retrofitted by GFRP and CFRP materials.

5.1 Specimens Strengthened for Shear

To conveniently investigate the performance of LWC beams shear-strengthened with FRP composites, the following simple superposition approach is adopted to evaluate shear capacity V_u of the shear-strengthened beams:

$$V_u = V_c + V_s + V_f, \tag{1}$$

where shear resistance of the concrete and longitudinal steel reinforcements V_c and shear capacity of transverse steel reinforcements V_s can be obtained from the test results of control beams or calculated via various existing design equations for RC structures. The accurate prediction of FRP shear contribution V_f is a key issue for the development of design guidelines.

Three design codes for NWC, namely, ACI 440.2R-17 (ACI, 2017), the Egyptian Code of Practice (ECP, 2005), and International Federation for Structural Concrete *fIB*-TG9.3 (FIB, 2001) were used to determine the shear capacity to calibrate the design equations in these resources with the experimental results in this study.

In (ECP, 2005), the nominal shear strength of the FRP shear reinforcement is given by

$$q_{fu} = A_f (E_f \varepsilon_{ef} / \gamma_f) (\sin \alpha + \cos \alpha) (d_f / d) / (S_f * b_w) \tag{2}$$

$$A_f = 2nt_f w_f \tag{3}$$

$$\varepsilon_{ef} = 0.75 \varepsilon_{fu}^* \leq 0.004 \tag{4}$$

$$\varepsilon_{fu}^* = CE \varepsilon_{fu} \tag{5}$$

Spacing S_f is less than either $d/4$ or 200 mm, whichever is smaller; this stipulation is also true for the width of the

FRP composites measured in the direction of the member axis.

In (ACI, 2017), the shear contribution of the FRP shear reinforcement is given by

$$V_f = \frac{A_{fv} F_{fe} (\sin\alpha + \cos\alpha) d_{fv}}{s_f}, \quad (6)$$

where

$$A_{fv} = 2nt_f w_f \quad (7)$$

The tensile stress in the FRP shear reinforcement at nominal strength is directly proportional to the level of strain that can develop in the FRP shear reinforcement at nominal strength:

$$F_{fe} = \epsilon_{fe} E_f \quad (8)$$

The effective strain in the FRP reinforcement is given by

$$\epsilon_{fe} = \min[k_v \epsilon_{fu}, 0.75 \epsilon_{fu}, 0.004], \quad (9)$$

where bond-reduction coefficient k_v is given by

$$k_v = \frac{k_1 k_2 L_e}{11900 \epsilon_{fu}} \leq 0.75 \quad (10a)$$

The bond-reduction coefficient relies on two modification factors, k_1 and k_2 , which account for the concrete strength and wrapping scheme, respectively. These modification factors are given by

$$k_1 = \left(\frac{f'_c}{27}\right)^{\frac{2}{3}}, \quad (10b)$$

where f'_c is the compressive strength of lightweight concrete, and

$$k_2 = \frac{d_{fv} - L_e}{d_{fv}}, \quad (10c)$$

where active bond length L_e is the length over which most of the bond stresses is maintained; this length is given by

$$L_e = \frac{23300}{(nt_f E_f)^{0.58}} \quad (10d)$$

In fib-TG9.3 (Fib, 2001), 2001, the shear capacity of a strengthened element is calculated according to the EC2 format as follows:

$$V_{Rd} = V_{cd} + V_{wd} + V_{fd}, \quad (11)$$

where FRP contribution to the shear capacity V_{fd} is given by

$$V_{fd} = 0.90 \epsilon_{f,e} E_{fu} \rho_f b_w d (\cot\theta + \cot\alpha) \sin\alpha \quad (12a)$$

$$\epsilon_{f,e} = \min \left[0.65 \left(\frac{f_{cm}^{2/3}}{E_{fu} \rho_f} \right)^{0.56} \times 10^{-3}, 0.17 \left(\frac{f_{cm}^{2/3}}{E_{fu} \rho_f} \right)^{0.30} \epsilon_{fu} \right] \quad (12b)$$

Fig. 14a shows a comparison between the experimental results and the three analytical models described above. Equations (2–5) (ECP, 2005) were used to compute q_{fu} , Eqs. (6–10) (ACI, 2017) were used to compute V_f , and Eqs. 11, 12a, 12b (FIB, 2001) were used to compute V_{fd} . The failure loads of each test beam specimen were predicted using the above design codes and compared with the measured experimental values. Since, these codes are not calibrated for the LWC beam, there will be a deviation of analytical models from experiment. This evident in Fig. 14. It can be seen from Fig. 14a that all the analytical models underestimate the prediction of failure loads compared to their counterparts obtained experimentally to different degrees. Fig. 14b presents the effect of the width of the GFRP and CFRP strips on the analytical results. It was noticed that the ACI 440.2R-17 (ACI, 2017) code is more compatible with the experimental results, while the ECP 208–2005 (ECP, 2005), FIB-TG9.3 (FIB, 2001) codes are more conservative.

5.2 Specimens Strengthened for Flexure

In ECP 208–2005 (ECP, 2005), determining the strain level in the FRP reinforcement at the ultimate moment of the cross section is important. The value of the strain permitted in FRP laminates at section failure (ϵ_{fe}) is governed by the strain level developed in the FRP at the point at which concrete crushes, the FRP ruptures, or the FRP debonds from the substrate. The value of this strain is calculated by

$$\epsilon_{fe} = \epsilon_{cu} \left(\frac{h - c}{c} \right) - \epsilon_{bi} \leq k_m \epsilon_{fu}^*, \quad (13)$$

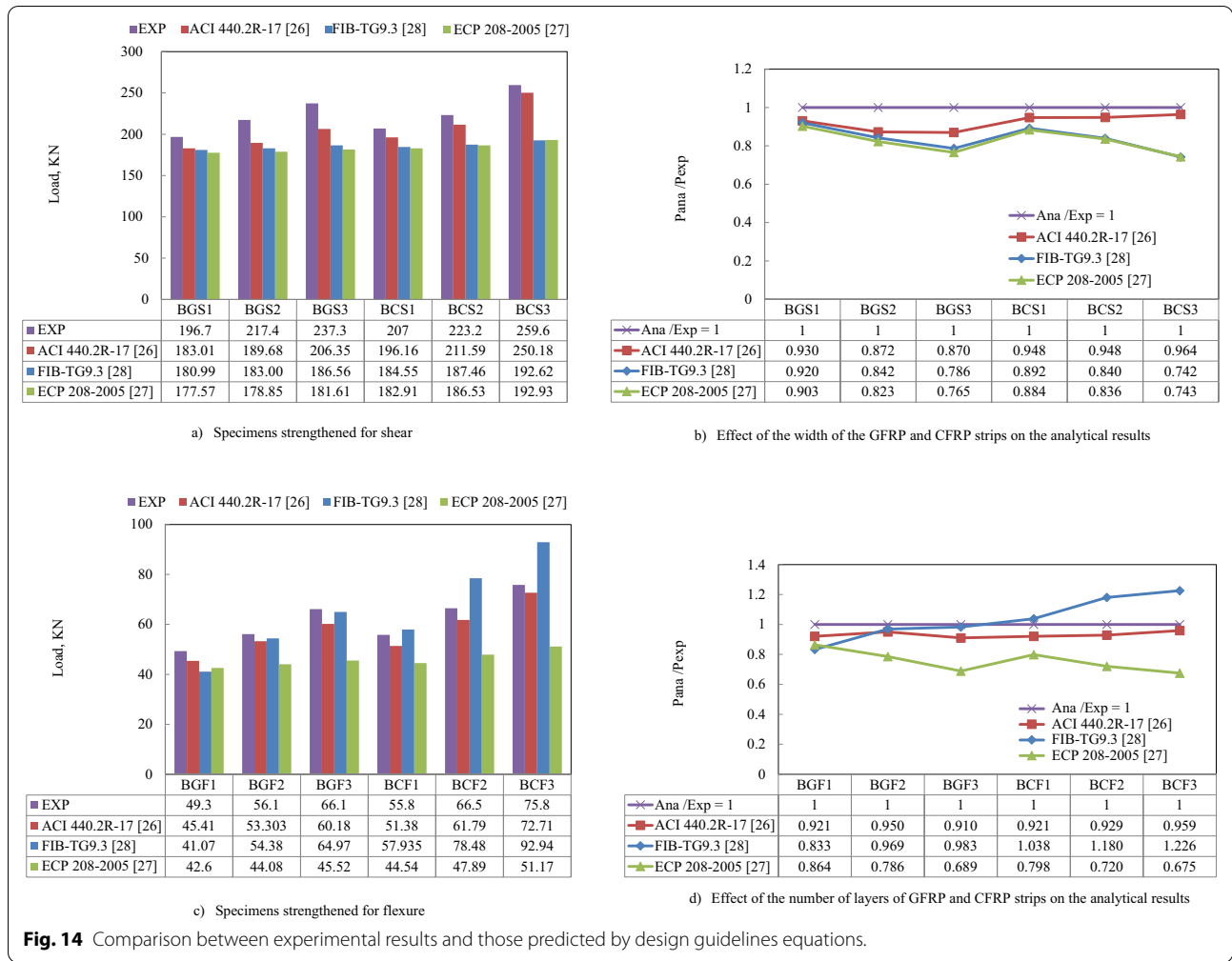
where

$$\epsilon_{fu}^* = CE \epsilon_{fu}, \quad (14)$$

And CE equals to 0.95.

$$f_{fe} = E_f \epsilon_{fe} / \gamma_f \quad (15)$$

The calculation procedure used to determine the ultimate flexural strength of the cross sections strengthened with externally bonded FRPs should satisfy the compatibility and equilibrium conditions and consider the governing failure mode. Such a procedure requires a trial-and-error method to ensure the compatibility and equilibrium requirements are satisfied. The values of the strains and stresses that develop in the reinforcing steel



are calculated by the following equations using a trial-and-error method:

$$\epsilon_s = (\epsilon_{fe} + \epsilon_{bi}) * \left(\frac{d - c}{h - c} \right) \tag{16}$$

$$f_s = E_s \epsilon_s \leq f_y / \gamma_s \tag{17}$$

The depth of the equivalent rectangular stress block of the compressed concrete is calculated by

$$a = \frac{A_s f_s + A_f f_{fe}}{(0.67 f_{cu} * b) / \gamma_c} \tag{18}$$

The ultimate flexural moment is calculated by

$$M_u = A_s f_s \left(d - \frac{a}{2} \right) + A_f f_{fe} \left(h - \frac{a}{2} \right) \tag{19}$$

The ultimate load P_u for two-point loading is calculated by

$$P_u = \frac{2M_u}{X} \tag{20}$$

where X is the distance between the supports and the loading point in mm. In ACI 440.2R-17 (ACI, 2017), according to the strain distribution, for any assumed depth to the neutral axis c , strain level in the FRP ϵ_f can be computed using the following:

$$\epsilon_f = \epsilon_{cu} \left(\frac{h - c}{c} \right) \leq \epsilon_{fu} \tag{21}$$

Stress level in the FRP f_f can be calculated from the strain level in the FRP, assuming elastic behaviour:

$$f_f = E_f \epsilon_f, \tag{22}$$

and strain level in steel under tension ϵ_s can be calculated by

$$\epsilon_s = \epsilon_f \left(\frac{d - c}{h - c} \right) \tag{23}$$

In addition, for steel under compression, the strain level can be calculated by

$$\epsilon_{s'} = \epsilon_f \left(\frac{d' - c}{h - c} \right) \tag{24}$$

Stress level in steel f_s is calculated from the strain level in steel, assuming elastic–plastic behaviour:

$$f_s = E_s \epsilon_s \tag{25}$$

Internal force equilibrium may be checked using

$$C = \frac{A_s f_s + A_f f_f + A_{s'} f_{s'}}{0.85 f_c \beta_1 b}, \tag{26}$$

where $\beta_1 = 0.8$ for concrete with a compressive strength of 35 MPa. Actual neutral axis depth c is found by simultaneously satisfying Eqs. 21, 24 and 26, thereby establishing the internal force equilibrium and strain compatibility. The nominal flexural strength of the section with FRP external reinforcement M_u can be computed using

$$M_u = A_s f_s \left(d - \frac{\beta_1 c}{2} \right) + \Psi A_f f_f \left(h - \frac{\beta_1 c}{2} \right) + A_{s'} f_{s'} \left(d' - \frac{\beta_1 c}{2} \right), \tag{27}$$

where $\Psi = 0.85$. Ultimate load P_u for two-point loading is calculated by

$$P_u = \frac{2M_u}{X} \tag{28}$$

In *fib*-TG9.3 (FIB, 2001), according to the steel yielding/concrete crushing failure mode, which is the most desirable mode, failure of the critical cross section occurs by the tensile steel reinforcement yielding followed by concrete crushing, while the FRP remains intact. The design bending moment of the strengthened cross section is calculated based on RC design principles. First, neutral axis depth x is calculated from the strain compatibility and internal force equilibrium, and then the design moment is determined based on the moment equilibrium. The analysis should consider that the RC element may not be fully unloaded when strengthening occurs, and hence, initial strain ϵ_0 in the extreme tensile fibre should be considered. The design bending moment capacity can be calculated using the following approach.

1. Calculate neutral axis depth x as follows:

$$0.85 \psi f_{cd} b x + A_{s2} E_s \epsilon_{s2} = A_{s1} f_{yd} + A_f E_f \epsilon_f, \tag{29}$$

where $\psi = 0.8$ and

$$\epsilon_{s2} = \epsilon_{cu} \frac{x - d_2}{x} \tag{30}$$

and ($E_s \epsilon_{s2}$ not to exceed F_{yd})

$$\epsilon_f = \epsilon_{cu} \frac{h - x}{x} - \epsilon_0 \tag{31}$$

2. Design the bending moment capacity as follows:

$$M_{Rd} = A_{s1} f_{yd} (d - \delta_G x) + A_f E_f \epsilon_f (h - \delta_G x) + A_{s2} E_s \epsilon_{s2} (\delta_G x - d_2), \tag{32}$$

where $\delta_G = 0.4$. Ultimate load P_u for two-point loading is calculated by

$$P_u = \frac{2M_{Rd}}{X} \tag{33}$$

Fig. 14c shows a comparison between the experimental results and the three analytical models obtained from the design codes. Equations (13–20) (ECP 208–2005) (ECP, 2005), Eqs. 21–28 ACI 440.2R-17 (ACI, 2017), and Eqs. 29–33 (FIB-TG 9.3) (FIB, 2001) were used to compute the flexural moment and failure loads of the strengthened specimens. The failure loads of the test beam specimens were predicted by the design codes for NWC and compared with the measured values for LWC. While Fig. 14d shows the accuracy of the analytical models when taking the number of layers into consideration for GFRP and CFRP vs the experimental results. It can be noticed from Fig. 14c, d that the ACI 440.2R-17 (ACI, 2017), FIB-TG9.3 (FIB, 2001) codes are more compatible with the experimental results, while the ECP 208–2005 code (ECP, 2005) is more conservative in predicting the ultimate load and it is not accurate in predicting the failure load when taking the number of FRP layers into account.

6 Conclusions

The effect of strengthening of LWC beams containing polystyrene beads using GFRP and CFRP laminates on the flexural and shear behaviour of studied beams was evaluated experimentally. The studied parameters were varying width of FRP wrapping for shear and number of FRP layers for flexure. In addition, the equations

currently used in the design codes were compared with the experimental work to check their validity for LWC beams strengthened using FRP laminates. The conclusions drawn from this study are as follows:

1. The increase in the width of the GFRP and CFRP strip had a significant impact on the loading capacity. LWC Beams strengthened for flexure showed an increase in load carrying capacity and deflection-hardening response. As a result, the strengthening of LWC beams using GFRP and CFRP improves loading capacity and ductility.
2. For shear strengthening LWC beams, it is recommended to use the maximum width of FRP.
3. The use of GFRP and CFRP strengthening techniques slows or stops the growth of cracks, delays initial cracking, lowers stiffness deterioration due to residual deflection, and increases the fatigue life of LWC beams. CFRP, on the other hand, is the best option for strengthening LWC beams.
4. The increased strain, number of fractures, and loading capacity caused by FRP strengthening do not modify the mode of failure. However, LWC beams were exhibiting visible sign through deformation at the verge of failure.
5. It's also possible to deduce that the number of layers in GFRP laminates is more effective than in CFRP laminates. On the other hand, all beams strengthened through GFRP and CFRP demonstrate deflection-hardening, reduction in crack width, and longitudinal steel strains.
6. With increasing the widths of strengthening strips or the number of strengthening layers, the longitudinal steel strain and stirrups' strain reduced. Furthermore, CFRP flexure strengthening is more effective than shear strengthening in lowering longitudinal steel strains. When GFRP laminates are compared to CFRP laminates, the effect of increasing the number of FRP layers is more important in lowering longitudinal strain.
7. For the experimental work carried out in this study, predicted results using ACI 440.2R-17 (ACI, 2017) design code equations were in close agreement to the shear specimens' experimental results, while the ECP 208–2005 (ECP, 2005) and *f*B-TG9.3 codes (FIB, 2001) were more conservative. The situation was different for flexure specimens that the ACI 440.2R-17 (ACI, 2017), *f*B-TG9.3 design codes (FIB, 2001) were more compatible with the experimental results, while the ECP 208–2005 (ECP, 2005) code was more conservative.

Abbreviations

A_{fr} , A_{fv} : Area of FRP external reinforcement; A_s : Total area of longitudinal steel reinforcement; b_f : The width of FRP; b_w : Width of concrete section; CE: Environmental reduction factor; d , d_{iv} : Effective depth of the concrete section; d' : Distance from centroid of compressive steel to upper face of member; d_f : Depth of FRP shear reinforcement; E_f , E_{fr} : Tensile modulus of elasticity of FRP; E_s : Modulus of elasticity of steel; f_c , f_{cm} , f_c' , f_{cd} , f_{cu} : Cube compressive strength of concrete; f_{fe} , f_f : Tensile strength of the FRP; f_y , f_s : Steel yield strength; h : Depth of concrete beam; h_f : Distance from extreme compression fibre to centroid of tension reinforcement; n : Number of plies of FRP reinforcement; k_1 , K_2 : Modification factors; K_v : The bond-reduction coefficient; L_e : The active bond length; q_{fr} : The nominal shear strength of the FRP shear reinforcement; S_f : Spacing of FRP shear reinforcement (distance between the centreline of the strips); t_f : Nominal thickness of one ply of the FRP reinforcement; V_u : The shear capacity of the shear strengthened reinforced concrete (RC) beam; V_c : The shear resistance of the concrete and longitudinal steel reinforcements; V_s : The shear capacity of transverse steel reinforcements or bent-up steel bars; V_f : The accurate prediction of the FRP shear contribution; w_f : Width of the FRP reinforcing plies; ϵ_{fr}^* : Maximum strain in the FRP; ϵ_f , ϵ_{fe} : FRP strain; ϵ_{bf} : Initial strain in concrete at the level of the FRP at service load level when installing the FRP; ϵ_s : Strain of the steel reinforcement; ϵ_{cu} : Ultimate concrete strain; ϵ_{ef} : Effective strain in FRP reinforcement; γ_f : Material strength reduction factor of FRP shear reinforcement; γ_s : Material safety factor for the steel reinforcement; γ_c : Material safety factor for the concrete; ρ_f : FRP reinforcement ratio; θ : Angle of diagonal crack with respect to the member axis; α : Angle of inclination of FRP reinforcement to the longitudinal axis of the member; β_1 : Coefficient accounting for the bond characteristics of the reinforcement; ψ : Load combination factor, or stress block area coefficient; δ_G : Stress block centroid coefficient.

Acknowledgements

Not applicable

Author contributions

WM: supervising the research, participating in writing and reviewing it. IS: writing the article, sharing in the theoretical work and sharing in the final revision. AZ: preparing the research plan and sharing in the final revision. SK: participation in the theoretical work, reviewing the discussion section, and sharing in the final revision. MS: carrying out the experimental work. All authors read and approved the final manuscript.

Authors' informations

Wael M. Montaser, BSc, MSc, PhD, Associate Professor, Head of Construction and Building Department; Ibrahim G. Shaaban, BSc, MSc, PhD, MICE, CEng, MStructE, FICE, FStructE, SFHEA, Reader of Civil Engineering; Amr H. Zaher, BSc, MSc, PhD, Professor of Concrete Structures; Sadaqat U. Khan, BSc, MSc, PhD, Professor Mustafa N. Sayed BSc, MSc, Assistant Lecturer.

Funding

Open access funding provided by The Science, Technology & Innovation Funding Authority (STDF) in cooperation with The Egyptian Knowledge Bank (EKB). Not applicable.

Availability of data and materials

All data generated or analysed during this study are included in this published article.

Declarations

Competing interests

The authors declare that they have no competing interests.

Author details

¹Construction and Building Department, Faculty of Engineering, October 6 University, Giza, Egypt. ²School of Computing and Engineering, University of West London, St Mary's Road, Ealing, W5 5RF London, UK. ³Structural Engineering Department, Faculty of Engineering, Ain Shams University, Cairo, Egypt. ⁴Department of Civil Engineering, Thar Institute of Sciences and Technology NED University of Engineering & Technology, Karachi, Pakistan.

Received: 28 January 2022 Accepted: 5 July 2022
Published online: 09 August 2022

References

- ACI. (2017). *Guide for the design and construction of externally bonded FRP systems for strengthening concrete structures*. American Concrete Institute.
- Agrawal, Y., Gupta, T., Sharma, R., Panwar, N. L., & Siddique, S. (2021). A Comprehensive review on the performance of structural lightweight aggregate concrete for sustainable construction. *Construction Materials*, 1(1), 39–62.
- Al-Allaf, M. H., Weekes, L., & Augustus-Nelson, L. (2019). Shear behaviour of lightweight concrete beams strengthened with CFRP composite. *Magazine of Concrete Research*, 71(18), 949–964.
- Aljaafreh, T. (2016). Strengthening of lightweight reinforced concrete beams using carbon fiber reinforced polymers (CFRP), MSc Thesis submitted to the University of Texas at Arlington, 74pp.
- Alhaddad, M. S., Binyahya, A. S., Alrubaidi, M., & Abadel, A. A. (2021). Seismic performance of RC buildings with Beam-Column joints upgraded using FRP laminates. *Journal of King Saud University-Engineering Sciences*, 33(6), 386–395.
- Al-Jelawy, H. (2013). Experimental and numerical investigations on bond durability of CFRP strengthened concrete members subjected to environmental exposure. *MSc Thesis*. University of Central Florida. <https://stars.library.ucf.edu/etd/2730>.
- Al-Jelawy, H. M., & Mackie, K. R. (2020). Flexural behavior of concrete beams strengthened with polyurethane-matrix carbon-fiber composites. *Journal of Composites for Construction*, 24(4), 04020027.
- Al-Jelawy Haider, M., & Mackie Kevin, R. (2021). Durability and failure modes of concrete beams strengthened with polyurethane or epoxy CFRP. *Journal of Composites for Construction*, 25, 04021021.
- Alshannag, M. J., & Alshenawy, A. O. (2021). Enhancing the flexural performance of lightweight reinforced concrete beams exposed to elevated temperatures. *Ain Shams Engineering Journal*. <https://doi.org/10.1016/j.asej.2020.12.020>
- Attari, N., Amziane, S., & Chemrouk, M. (2012). Flexural strengthening of concrete beams using CFRP, GFRP and hybrid FRP sheets. *Construction and Building Materials*, 37, 746–757.
- Danraka, M. N., Mahmud, H. M., Oluwatosin, O. K. J., & Student, P. (2017). Strengthening of reinforced concrete beams using FRP technique: a review. *International Journal of Engineering Science*, 7(6), 13199.
- ECP. (2005). *Egyptian code of practice for the use of fiber reinforced polymer (FRP) in the construction fields* Ministry of Housing, Utilities and Urban Utilities.
- ECP (Egyptian Code of Practice) (2018) ECP 203-2018: Design and Construction for Reinforced Concrete Structures. Ministry of Building Construction, Research Center for Housing, Building and Physical Planning, Cairo, Egypt.
- FIB. (2001). *Externally bonded FRP reinforcement for RC structures* (p. 138). International Federation for Structural Concrete (FIB).
- Kim, S.-H., Park, J.-S., Jung, W.-T., Kim, T.-K., & Park, H.-B. (2021). Experimental study on strengthening effect analysis of a deteriorated bridge using external prestressing method. *Applied Sciences*, 11(6), 2478.
- Kotwal, S. S., Pati, S. A., More, M. M., & Adure, S. G. (2017). Comparison experimental & analytical results of lightweight reinforced concrete beam strengthened with GFRP strips, international journal of innovative research in science. *Engineering and Technology*, 6(1), 7.
- Maraq, M. A. A., Tayeh, B. A., Ziara, M. M., & Alyousef, R. (2021). Flexural behavior of RC beams strengthened with steel wire mesh and self-compacting concrete jacketing—experimental investigation and test results. *Journal of Materials Research and Technology*, 10, 1002–1019.
- Naji, A. J., Al-Jelawy, H. M., Saadon, S. A., & Ejel, A. T. (2021). Rehabilitation and strengthening techniques for reinforced concrete columns. *Journal of Physics Conference Series*, 1895(1), 012049.
- Newman, J., & Owens, P. (2003). Properties of lightweight concrete. *Advanced Concrete Technology*, 3, 1–29.
- Önal, M. M. (2014). Strengthening reinforced concrete beams with CFRP and GFRP. *Advances in Materials Science and Engineering*. <https://doi.org/10.1155/2014/967964>
- Panahi, M., Zareei, S. A., & Izadic, A. (2021). Flexural strengthening of reinforced concrete beams through externally bonded FRP sheets and near surface mounted FRP bars. *Case Studies in Construction Materials*. <https://doi.org/10.1016/j.cscm.2021.e00601>
- Ramesh, G., Srinath, D., Ramya, D., & Krishna, B. V. (2021). Repair, rehabilitation and retrofitting of reinforced concrete structures by using non-destructive testing methods. *Materials Today: Proceedings*. <https://doi.org/10.1016/j.matpr.2021.02.778>
- Shaaban, I. G., & Seoud, O. A. (2018). Experimental behavior of full-scale exterior beam-column space joints retrofitted by ferrocement layers under cyclic loading. *Case Studies in Construction Materials*, 8, 61–78.
- Shaaban, I. G., Zaher, A. H., Said, M., Montaser, W., Ramadan, M., & AbdElhameed, G. N. (2020). Effect of partial replacement of coarse aggregate by polystyrene balls on the shear behaviour of deep beams with web openings. *Case Studies in Construction Materials*, 12, e00328.
- Shannag, M. J., Al-Akhras, N. M., & Mahdawi, S. F. (2014). Flexure strengthening of lightweight reinforced concrete beams using carbon fibre-reinforced polymers. *Structure and Infrastructure Engineering*, 10(5), 604–613.
- Sundarraja, M., & Rajamohan, S. (2009). Strengthening of RC beams in shear using GFRP inclined strips—an experimental study. *Construction and Building Materials*, 23(2), 856–864.
- Valivonis, J., & Skuturna, T. (2007). Cracking and strength of reinforced concrete structures in flexure strengthened with carbon fibre laminates. *Journal of Civil Engineering and Management*, 13(4), 317–323.
- Vishakh, T. M., & Vasudev, R. (2018) "Lightweight Aggregate Concrete using Expanded Polystyrene Beads-A Review", International Research Journal of Engineering and Technology (IRJET), Vol. 5, No. 11, pp. 924-928, <https://www.irjet.net/archives/V5/i11/IRJET-V5I11177.pdf>

Publisher's Note

Springer Nature remains neutral with regard to jurisdictional claims in published maps and institutional affiliations.

Submit your manuscript to a SpringerOpen® journal and benefit from:

- Convenient online submission
- Rigorous peer review
- Open access: articles freely available online
- High visibility within the field
- Retaining the copyright to your article

Submit your next manuscript at ► [springeropen.com](https://www.springeropen.com)